Advanced processing of a novel acquisition from offshore Cyprus

Monica Hartmann, Chase Asher, Scott Braquet, Jana Caskey, Naila Samai, DUG Technology; Ares Ouzounis, ExxonMobil Technology & Engineering Company*

Summary

New acquisition technologies enhance subsurface imaging but can introduce new challenges. In 2022, a novel acquisition was undertaken off the coast of Cyprus. It included a blended dual-vessel rich azimuth acquisition using multi-component streamers and sources consisting of single large-volume airguns. The goal was to improve azimuthal information and enhance low-frequencies compared to more traditional narrow azimuth streamer acquisition. The enhanced bandwidth and azimuthal content would benefit the derivation of velocities in this geologically complex basin through the use of full-waveform inversion (FWI). Ensuring the preservation of the bandwidth through inversion-based deblending and improving our understanding of the source wavelet through source inversion would provide the best inputs for FWI, but the presence of complex geological features with varying elastic properties generated converted wave energy, complicating imaging efforts. This paper details the advanced processing techniques applied to realize the benefits of this new acquisition technology and enhance subsurface imaging in the presence of geologic complexity.

Introduction

The Herodotus Basin, located in the eastern Mediterranean Sea, is bordered by the island of Cyprus to the north and the Levantine Basin to the east. It has a complex geological history, highlighted by the Messinian Salinity Crisis, during the late Miocene, approximately 6 million years ago. During this period, the Mediterranean Sea nearly desiccated due to the closure of its connection with the Atlantic Ocean, resulting in the formation of extensive salt deposits. The salt geometry can vary from simple, consisting of two horizons, to highly deformed sequences of overhangs accompanied by intra-salt reflectivity (El-Bassiony et al., 2018). Frontier exploration in the basin is challenged by illumination issues due to the complex salt.

Acquisition

To overcome these challenges, in 2022, a rich azimuth dataset was acquired with two source vessels sailing at a crossline offset of 1400 m. Each vessel was equipped with two large-volume single airgun sources to improve low-frequency information and eliminate directivity effects due to angle or azimuth compared to traditional airgun arrays, benefiting FWI (Udengaard, 2023). The airgun consisted of two 4000 cu. in. chambers connected to provide 8000 cu. in. volume operating at 2000 psi. This large source volume extended the usable low frequencies and improved the signal-to-noise content compared to an older conventional source acquisition nearby (Ou et al., 2023). In the post-salt, the data was over 9 dB higher in amplitude at 3 Hz (Figure 1).

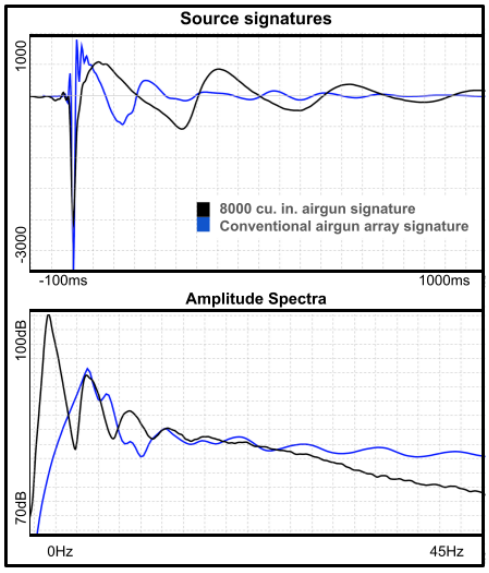

Figure 1: The source signature of the large-volume airgun is displayed in black, with the signature of an older conventional survey acquired nearby in blue. Beneath is a comparison of the signatures' amplitude spectra illustrating the additional low-frequency content and large bubble effects of the larger volume airgun.

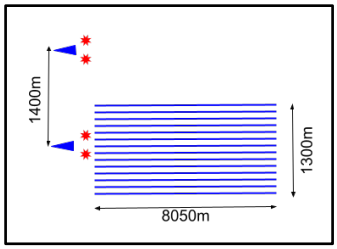

Figure 2: The dual-vessel rich azimuth acquisition configuration.

The recording vessel towed 14 x 100 m x 8050 m cable spread (Figure 2). The dual sensor cables, which record both the pressure and the vertical component of particle velocity, were towed at a depth of 20 meters, reducing the impact of noise due to waves and weather. These components can be

combined to separate the up-going and down-going wavefields, thus removing the receiver side ghost.

The acquisition was designed to balance the need for increased azimuthal coverage while remaining within economical constraints. Although ocean-bottom node (OBN) data have been proven to improve imaging in salt basins, such a high effort survey can be cost prohibitive for large exploration acreage. During acquisition design, it was determined that one additional source vessel abreast of the streamer vessel would provide additional illumination to better image subsalt plays, while further additional source vessels provided only modest improvement compared to their cost (Tapie et al., 2023).

Traveling at 4 knots, the vessels were able to refill the sources to the desired pressure firing every 25m. By alternating firing between vessels, a 12.5m shot interval was achieved with 5 seconds of clean recording. The blended acquisition improved the offset sampling and acquisition efficiency. The lower cost of blended seismic surveys and shorter acquisition times can result in the faster maturation of drillable prospects (Ou et al., 2016). The survey design led to enhanced low frequencies and high signal-to-noise compared to acquisition with conventional sources and increased azimuth over narrow azimuth (NAZ) surveys previously acquired in the area; all of which improved illumination of subsalt plays.

Pre-processing

Due to this survey's shot spacing and the characteristics of the recorded wavefield, the multiples of the previous shot overlapped (in time) with the primary reflection signal. Hence, separating the energy from the various overlapping shots was a crucial first step in the data processing. An iterative-relaxation inversion algorithm that gradually reconstructs unblended data from blended shots was used (Kumar et al., 2020).

Since inversion deblending needs to explain all of the input data as a blending of the deblended shot records, we must be able to create continuous records which necessitates minimally processed input data. Pressure and particle velocity were deblended separately. Ensuring that the primary signals are preserved while separating the blended energy is especially important in this subsalt environment where little high-frequency signal penetrates the salt (Peng 2016). Figure 3 a) demonstrates the effective creation of the up-going wavefield (using both sensor components) after deblending, b) and c) show the strong interference of the subsequent energy on the hydrophone and geophone data.

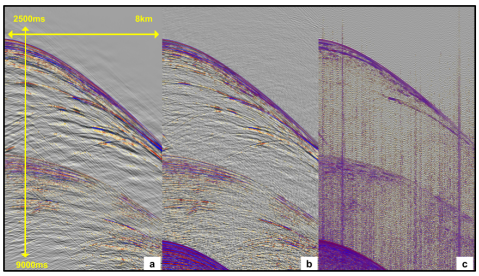

Figure 3: a) Up-going wavefield after deblending of both components; b) hydrophone and c) geophone data before deblending with a 20 Hz low cut filter applied to reduce mechanical noise in the display.

FWI

A critical step for successful imaging in complex geological regions is the derivation of an accurate velocity model. FWI enables the determination of high-resolution velocity models but is sensitive to the source signature used for modelling. To ensure the estimation of a robust, true-amplitude signature, a least-squares matching approach on the direct arrival of the modeled and observed data was employed. Accurately matching the direct arrivals would enhance the fidelity of the modeled seismic data during the inversion process.

Single parameter FWI (SP-FWI), using reflections, and a density field related to velocity based on a well near the survey, was performed at 3, 5 and 7 Hz (3 dB down) in the post-salt to update Vp. Prior to salt interpretation, an additional pass of tomography was applied to correct for the leakage of elastic effects at the top salt interface. After interpretation, intra-salt SP-FWI refined velocities to account for inclusions. Reflection tomography using reverse-time migration surface-offset gathers (RTM SOGs) was used to complete the velocity model pre-salt. Figure 4a) illustrates the geologic conformability of the updated velocity model. In b) the high signal-to-noise content of the observed data, even at 3 Hz, can be seen, and c) indicates the clear conformability of the caprock and salt on the modeled and synthetic at 7 Hz.

Converted-wave attenuation

Despite efforts in acquisition design to enhance illumination, we found that high-amplitude converted wave energy at the salt boundaries obscured parts of the subsalt stratigraphy (Ogilvie and Purnell, 1996). By employing a dual-leg 3D visco-acoustic forward modeling approach, we generated kinematically accurate data domain models for the PSPP and PPSP arrivals. The kinematics of different converted wave modes from a known reflector can be modeled by assigning different velocities for background and scattered energy,

representing P- and S-velocities (Huang et al., 2013; Kumar et al., 2018; Hartmann et al., 2024). S-velocities were derived by scaling the salt section of the P-velocity based on the Vp/Vs ratio from a nearby well. Two forward modeling simulations were conducted to create just the PSPP and PPSP noise models, as the PSSP energy was much lower in amplitude than the primary and other converted wave modes. The PSSP energy was not visible in the stack sections and showed higher curvature than the primaries, allowing it to be effectively addressed with a pre-migration high-resolution parabolic radon technique.

Due to the acoustic nature of the modeling engine the noise model of the converted wave reflection exhibits different amplitude variation with angle (AVA) compared to the recorded data. An elastic propagator would have provided more accurate kinematics and dynamics but at a significantly higher computational cost. To address this, adaptive subtraction of the converted wave noise model is necessary, which can be performed in either the data domain or the image domain. In this workflow, pre-migration least-squares t-x global matching was applied in the common channel domain to the PPSP and PSPP models separately, which were then bottom-muted based on onset arrival times. This was followed by adaptive local matching operating simultaneously on both noise models in the shot domain, with an additional joint match in the common midpoint (CMP) domain with normal moveout applied to flatten and preserve primary reflections. The matched models were then subtracted to attenuate the PSPP and PPSP converted wave energy from the deghosted and demultipled shot records before the RTM.

In the Kirchhoff pre-stack depth migration (preSDM) 15° to 30° angle stack section, prior to converted wave removal, a high amplitude event can be seen obscuring the subsalt primary reflectors (Figure 5a). Although this energy is parallel to nearby primaries, it has been well attenuated using the described workflow (Figure 5b). In the Kirchhoff preSDM image gathers, the energy of the base of salt primary P-wave reflection decreases from 15° onwards, highlighted by the yellow oval. At the same offsets, a converted wave event just below the base of salt has increased in amplitude. Deviation from primary curvature and lack of amplitude at low incidence angles compared to primaries can be observed (Figure 5c). The image gathers clearly show effective separation and attenuation of the converted wave noise from the P-wave image (Figure 5d).

Imaging

Due to the complex nature of the salt overburden, ray-based imaging methods were deemed insufficient for pre-salt imaging. For final migrations, it was decided to use RTM (32.5 Hz at 3dB) and include SOGs for the creation of angle stacks (18 Hz at 3dB). The migration of SOGs allowed for additional post-migration processing in the common-depth point (CDP) domain, including residual moveout correction, demultiple and additional denoise subsalt.

Conclusions

Blended rich azimuth acquisition using multi-component streamers and large-volume single airgun sources significantly reduced acquisition time, improved azimuthal information, and enhanced low-frequency data in this complex geologic setting. This paper demonstrated the successful recovery of the deblended signal and attenuation of receiver ghost using multi-component data. The improved understanding of the source signature through inversion optimized FWI performance and maximized the benefit of extended low-frequency bandwidth. This aided velocity model building and imaging in the challenging subsalt environment offshore Cyprus, with the incorporation of converted wave modeling to prevent contamination of the final image.

Acknowledgments

Many thanks to ExxonMobil, the Cyprus government, and the management of DUG Technology for their collaboration and permission to publish this paper.

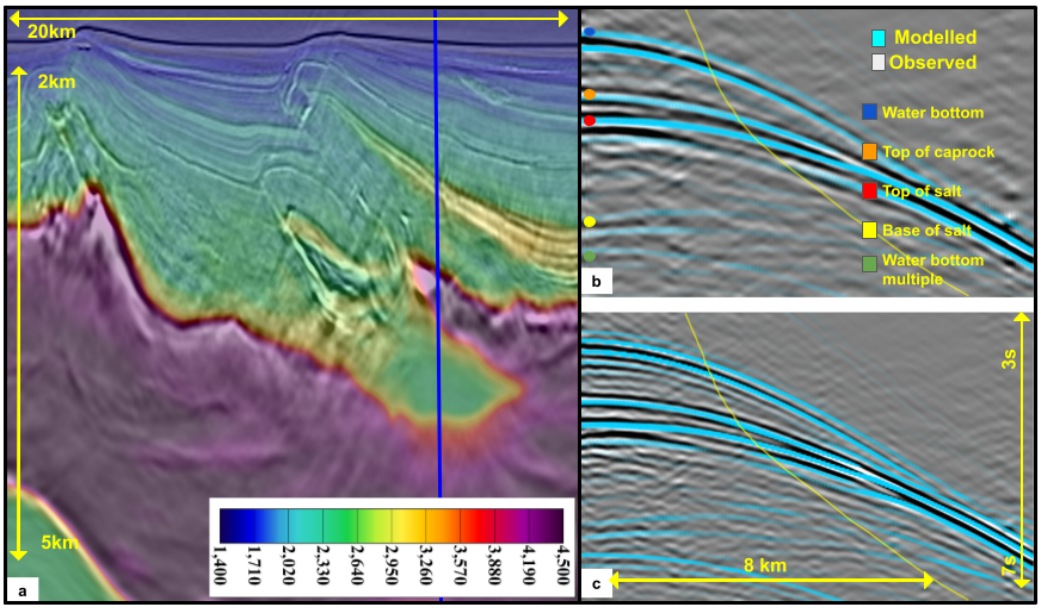

Figure 4: a) The final 45 Hz RTM stack with SP-FWI derived velocity overlain. The shot shown is marked by the blue line. b) The modeled (blue) and observed (white) shot at 3 Hz using the final velocities with the SP-FWI mute in red. Notice the significant signal at this low frequency. c) The modeled (blue) and observed (white) shot at 7 Hz with a 35 degree mute in yellow.

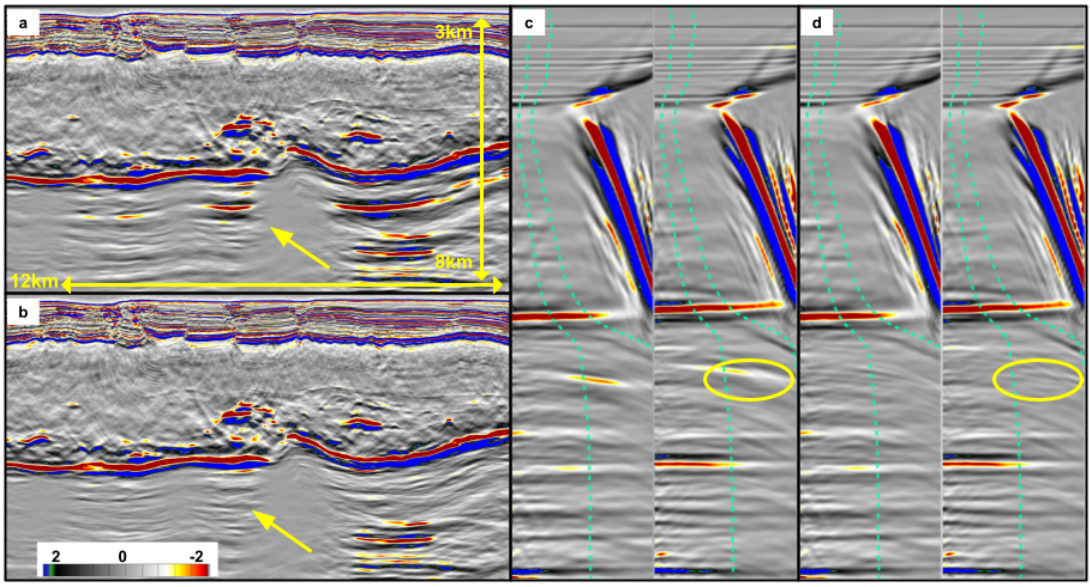

Figure 5: a,b) Kirchhoff PreSDM mid-angle stack before and after converted wave removal; c,d) Kirchhoff PreSDM gathers before and after converted wave removal with the mid-angle stacks displayed in green.